

Gallium Oxide Nanorods: Novel, Template-Free Synthesis and High Catalytic Activity in Epoxidation Reactions**

Warunee Lueangchaichaweng, Neil R. Brooks, Sonia Fiorilli, Elena Gobechiya, Kaifeng Lin, Li Li, Sonia Parres-Esclapez, Elsa Javon, Sara Bals, Gustaaf Van Tendeloo, Johan A. Martens, Christine E. A. Kirschhock, Pierre A. Jacobs, and Paolo P. Pescarmona*

Abstract: Gallium oxide nanorods with unprecedented small dimensions (20–80 nm length and 3–5 nm width) were prepared using a novel, template-free synthesis method. This nanomaterial is an excellent heterogeneous catalyst for the sustainable epoxidation of alkenes with H_2O_2 , rivaling the industrial benchmark microporous titanosilicate TS-1 with linear alkenes and being much superior with bulkier substrates. A thorough characterization study elucidated the correlation between the physicochemical properties of the gallium oxide nanorods and their catalytic performance, and underlined the importance of the nanorod morphology for generating a material with high specific surface area and a high number of accessible acid sites.

One-dimensional nanomaterials such as nanorods and nanowires are drawing growing attention for the specific physical properties that they display compared to their bulk counterparts.^[1] For a surface-related application such as heterogeneous catalysis, a key advantage of nanomaterials is provided by the increased surface-to-volume ratio that accompanies the decrease in the size of the catalyst particles.

Additionally, the surface of one-dimensional nanomaterials is inherently rich in coordinatively unsaturated sites that can play an active role in catalytic reactions. Solution-phase techniques have been shown to be a very advantageous and viable approach for the preparation of metal-oxide nanomaterials.^[2] However, these methods typically require the use of templates or other additives to direct the growth of the material towards a specific morphology.

Herein, we present a novel and straightforward method for the fabrication of gallium oxide nanorods with unprecedented small dimensions (length ≤ 80 nm). This nanomaterial displays excellent properties as heterogeneous catalyst for the epoxidation of alkenes using the environmentally friendly hydrogen peroxide as the oxidant.

Gallium oxide nanorods (Ga_2O_3 -NR) were prepared using a precipitation method involving solvolysis of $GaCl_3$ with 2-butanol, followed by hydrolysis and condensation of the formed species (Figure 1A). The method is reliable and accessible, does not require any expensive template or additive, is carried out at very mild temperature and no energy-consuming calcination step is needed prior to catalytic application (see the Supporting Information for the detailed synthesis procedure). The material presents rod-like morphology with a length varying from 20 to 80 nm and a width of 3–5 nm (Figure 1B,C). The X-ray diffractogram of the nanorods displays two broad peaks (Figure 1F), which are slightly shifted compared to those of a γ - Ga_2O_3 sample prepared as a reference (γ - Ga_2O_3 -lit).^[3] Although the broadened diffraction peaks of Ga_2O_3 -NR suggest a low crystallinity, a well-defined local structural order was evidenced by high-resolution transmission electron microscopy (HR-TEM) and selected area electron diffraction (SAED) (Figure 1D,E): the observed planes correspond to the XRD reflections and match well the d spacings and the orientation of the (100) and (105) planes of the seldom reported ϵ - Ga_2O_3 polymorph.^[4]

The nanorod morphology of Ga_2O_3 -NR results in the highest specific surface area ($192\text{ m}^2\text{g}^{-1}$) ever reported for a gallium oxide.^[3,5] The adsorption isotherm of type II with H_2 hysteresis loop (Figure S1A) indicates the presence of slit-shaped interparticle pores originating from packing of the nanorods.

The generation of nanorods is ascribed to an anisotropic structural feature of the intermediate species, most likely gallium oxyhydroxides, which are formed in the synthesis mixture. Indeed, gallium oxyhydroxides and their better known aluminum counterparts are characterized by orthorhombic unit cells, in which one cell parameter is much larger than the other two.^[6] The conversion of gallium oxyhydroxide

[*] W. Lueangchaichaweng, Dr. E. Gobechiya, L. Li, Dr. S. Parres-Esclapez, Prof. J. A. Martens, Prof. C. E. A. Kirschhock, Prof. P. A. Jacobs, Prof. P. P. Pescarmona
Centre for Surface Chemistry and Catalysis, University of Leuven
Kasteelpark Arenberg 23, Heverlee, 3001 (Belgium)
E-mail: paolo.pescarmona@biw.kuleuven.be

Dr. N. R. Brooks
Department of Chemistry, University of Leuven
Celestijnenlaan 200F, Heverlee, 3001 (Belgium)

Dr. S. Fiorilli
DISAT, Politecnico di Torino
Corso Duca degli Abruzzi 24, Torino, 10129 (Italy)

Prof. K. Lin
Natural Science Research Centre, Academy of Fundamental and Interdisciplinary Science, Harbin Institute of Technology
box-3026, 150080 Harbin (China)

Dr. E. Javon, Prof. S. Bals, Prof. G. Van Tendeloo
EMAT, University of Antwerp
Groenenborgerlaan 171, 2020 Antwerp (Belgium)

[**] This work was supported by START1, Methusalem, Prodex, IAP-PAI, and the ERC (grant number 24691—COUNTATOMS and grant number 335078—COLOURATOM) projects. The authors acknowledge Dr. K. Houthoofd, G. Vanbutsele, Dr. C. Klayson, Prof. J. W. Seo, Dr. T. Korányi, and Prof. K. Binnemans for their support in the characterizations, and Dr. C. Özdilek for useful scientific discussions.

Supporting information for this article is available on the WWW under <http://dx.doi.org/10.1002/anie.201308384>.

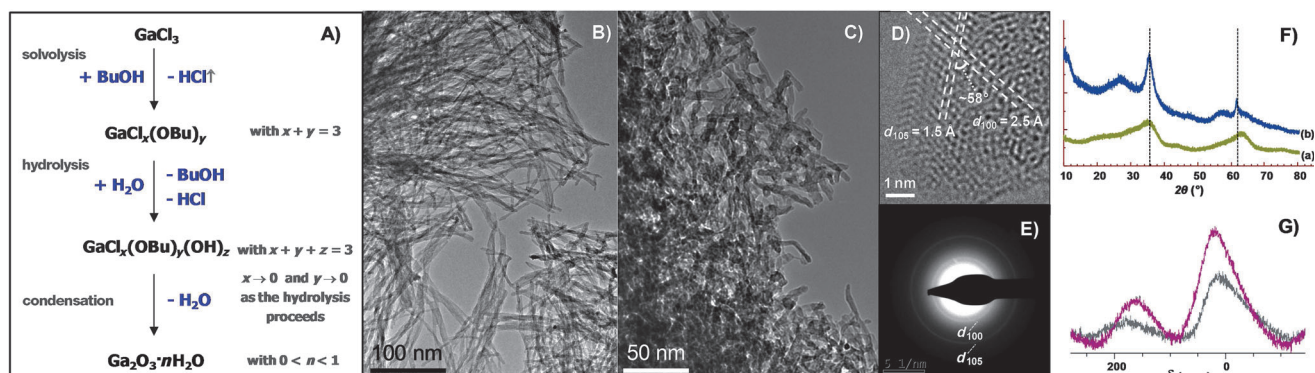


Figure 1. A) Scheme of the formation of $\text{Ga}_2\text{O}_3\text{-NR}$ (BuOH is 2-butanol). B, C) TEM images of $\text{Ga}_2\text{O}_3\text{-NR}$ with 40–80 nm length (B) and with 20–50 nm length (C). The size of the nanorods can be tuned by adjustments in the protocol of addition of H_2O (see the Supporting Information), without affecting the catalytic activity of the material. D) HR-TEM picture of a selected nanorod ($d_{105} = 1.5 \text{ \AA}$, $d_{100} = 2.5 \text{ \AA}$, and angle of 58°). E) Selected area electron diffraction pattern of $\text{Ga}_2\text{O}_3\text{-NR}$. F) XRD pattern of: $\gamma\text{-Ga}_2\text{O}_3\text{-lit}$ (a) and $\text{Ga}_2\text{O}_3\text{-NR}$ (b). The vertical lines correspond to reflections of the (100) and (105) planes of $\varepsilon\text{-Ga}_2\text{O}_3$. G) ^{71}Ga MAS NMR spectra of $\text{Ga}_2\text{O}_3\text{-NR}$ (gray) and $\gamma\text{-Ga}_2\text{O}_3\text{-lit}$ (violet), showing Ga in tetrahedral (ca. 150 ppm) and octahedral (ca. 0 ppm) coordination.

Table 1: Physicochemical properties of $\text{Ga}_2\text{O}_3\text{-NR}$ and $\gamma\text{-Ga}_2\text{O}_3\text{-lit}$.

Catalyst	Surface area [$\text{m}^2 \text{g}^{-1}$] ^[a]	$\text{Ga}_{\text{tetra}}:\text{Ga}_{\text{octa}}$ ^[b]	$n_{\text{H}_2\text{O}}$ nm^{-2} ^[c]	Acid sites [mmol g^{-1}] ^[d]	L:B ratio ^[d]	Density of acid sites (sites nm^{-2}) ^[d]
$\text{Ga}_2\text{O}_3\text{-NR}$	192	1:10	26	0.16	18:1	0.63
$\gamma\text{-Ga}_2\text{O}_3\text{-lit}$	98	1:5	36	0.06	only L	0.38

[a] Measured by N_2 physisorption. [b] Determined by ^{71}Ga MAS NMR spectroscopy. [c] Estimated by TGA. [d] Based on FTIR spectroscopy of adsorbed pyridine at 150°C . Prior to the IR measurement the samples were subjected to evacuation at 400°C , implying that the measured ratios of Lewis to Brønsted acid sites are expected to be higher than in the materials used as catalysts. The epoxidation activity of $\text{Ga}_2\text{O}_3\text{-NR}$ calcined at 400°C does not differ significantly from that of the as-synthesized material (see Table 2).

into oxide is expected to proceed through condensation steps followed by partial migration of Ga atoms from octahedral to tetrahedral sites.^[7] Accordingly, solid-state ^{71}Ga NMR spectroscopy of $\text{Ga}_2\text{O}_3\text{-NR}$ shows the presence of Ga atoms in both tetrahedral and octahedral coordination (Figure 1 G and Table 1), as encountered in $\varepsilon\text{-Ga}_2\text{O}_3$ and in other gallium oxide polymorphs,^[4] but in contrast to oxyhydroxide structures in which all metal atoms are octahedrally coordinated.^[8]

$\text{Ga}_2\text{O}_3\text{-NR}$ was tested as heterogeneous catalyst for the epoxidation of alkenes with aqueous H_2O_2 (Table 2). This is the preferential path to produce epoxides, which are a family of versatile compounds used in numerous industrial syntheses of fine chemicals.^[9] Ethyl acetate was employed as environmentally acceptable and inexpensive solvent. The catalytic performance of $\text{Ga}_2\text{O}_3\text{-NR}$ was compared both to $\gamma\text{-Ga}_2\text{O}_3\text{-lit}$ and to titanium silicalite 1 (TS-1, see Figure S2), which was chosen as benchmark because this zeolite is considered the optimum heterogeneous catalyst for the epoxidation of small and linear alkenes with H_2O_2 .^[10] Remarkably,

the epoxide yield achieved with $\text{Ga}_2\text{O}_3\text{-NR}$ in the conversion of a linear alkene such as 1-octene is comparable to that of TS-1, whereas the catalytic performance is much superior with bulky cyclic alkenes such as cyclohexene and cyclooctene, which are too large to diffuse through the micropores of TS-1. The almost complete epoxide selectivity achieved

Table 2: Catalytic epoxidation of selected alkenes using 50 wt% aqueous H_2O_2 (Y=yield and S=selectivity).

Alkene	Catalyst	Y_{epoxide} [%]	S_{epoxide} [%]	TON ^[a]	Productivity ^[b]
cyclooctene	$\text{Ga}_2\text{O}_3\text{-NR}$	84	> 99	266	5.3
	$\gamma\text{-Ga}_2\text{O}_3\text{-lit}$	14	> 99	109	0.9
	TS-1	0	0	—	0
	blank	1	> 99	—	—
	$\text{Ga}_2\text{O}_3\text{-NR}_{400^\circ\text{C}}$	79	> 99	250	5.0
1-octene	$\text{Ga}_2\text{O}_3\text{-NR}$	17	98	55	1.1
	$\gamma\text{-Ga}_2\text{O}_3\text{-lit}$	3	> 99	24	0.2
	TS-1	21	> 99	70	1.3
cyclohexene	$\text{Ga}_2\text{O}_3\text{-NR}$	45	> 99	142	2.2
	$\gamma\text{-Ga}_2\text{O}_3\text{-lit}$	13	> 99	104	0.6
	TS-1	0	0	—	0
styrene	$\text{Ga}_2\text{O}_3\text{-NR}$	20	58 ^[c]	109	1.2
	$\gamma\text{-Ga}_2\text{O}_3\text{-lit}$	7	44 ^[c]	109	0.4
	TS-1	6	23 ^[c]	87	0.4

Conditions: 2 mmol alkene, 4 mmol H_2O_2 , 40 mg of catalyst, 2.0 g of ethyl acetate as solvent (acetonitrile for the reactions with TS-1, see the Supporting Information), 4 h at 80°C . [a] TON ($\text{mol}_{\text{alkene converted}}/\text{mol}_{\text{active sites}}$) was calculated using the number of acid sites for $\text{Ga}_2\text{O}_3\text{-NR}$ and $\gamma\text{-Ga}_2\text{O}_3\text{-lit}$ (Table 1) and the number of Ti atoms for TS-1. [b] Productivity is defined as $g_{\text{epoxide}}/g_{\text{catalyst}}$. [c] The incomplete epoxide selectivity observed with styrene is due to the formation of benzaldehyde, which originates from the oxidative cleavage of the vinyl group.^[12]

with Ga₂O₃-NR for these alkenes is also noteworthy, particularly in the case of cyclohexene, which is rather prone to the formation of the diol and other side-products.^[11] In the epoxidation of styrene, Ga₂O₃-NR gave higher conversion and higher epoxide selectivity compared to TS-1. The crucial effect of the synthesis method on the catalytic performance of gallium oxides is demonstrated by the strikingly superior activity of Ga₂O₃-NR compared to γ -Ga₂O₃-lit (Table 2), in spite of having the same chemical composition.

The origin of the excellent catalytic properties of Ga₂O₃-NR was investigated through a combination of physicochemical characterization techniques. FTIR and Raman spectroscopy unequivocally demonstrate the activation of H₂O₂ by Ga₂O₃-NR: an IR signal at 835 cm⁻¹ and a clear Raman shoulder at higher wavenumber compared to the signal of physisorbed H₂O₂ at 877 cm⁻¹ appear in the spectra of H₂O₂ in contact with Ga₂O₃-NR, while these signals are not observed in the absence of H₂O₂ or if the inactive SiO₂ is impregnated with H₂O₂ (Figure 2A,B and Figure S3). We propose that the two signals stem from bidentate (η^2) Ga-hydroperoxide and Ga-peroxide species that can be interconverted upon water removal,^[13] which occurs in the Raman cell upon laser heating (see the Supporting Information). This assignment is supported by the similarity between the position and stability of the IR signal at 835 cm⁻¹ (Figure 2A) and the band generated by H₂O₂ activation on TS-1 (837 cm⁻¹), which was attributed to the O–O stretching of an η^2 -hydroperoxide.^[14] The proposal is also in line with the higher epoxide yield obtained over Ga₂O₃-NR with internal alkenes compared to terminal linear alkenes, evidencing a pathway in which H₂O₂ is activated to form a metal-hydroperoxide intermediate, followed by heterolytic cleavage of the O–O bond and transfer of an oxygen atom to the alkene (the double bond in internal alkenes is more electron-rich and thus more prone to undergo electrophilic attack by one of the O atoms).^[15] Moreover, a homolytic radical pathway is ruled out by the

negligible formation of products of allylic oxidation in the reaction of cyclohexene (Table 2).^[15]

The higher surface area of the nanorods compared to γ -Ga₂O₃-lit (Table 1) allows a better contact with the reagents, and its open structure prevents water entrapment that, on the other hand, can occur in the ink-bottle-shaped pores of γ -Ga₂O₃-lit (Figure S1B). These features result in the lower hydrophilicity of Ga₂O₃-NR, as demonstrated by the lower number of H₂O molecules adsorbed per square nanometer of surface (Table 1). Too high hydrophilicity is detrimental for the epoxidation as it would hinder the approach of the apolar alkene to the catalyst surface.^[16] The morphology of the nanorods is also favorable for the dispersion of the catalyst particles in solution,^[6b,17] in comparison with the large aggregates of particles lacking a specific morphology of γ -Ga₂O₃-lit (Figure S4). Although important, these surface and morphological properties cannot account alone for the remarkable superiority of the activity of Ga₂O₃-NR compared to γ -Ga₂O₃-lit.

The correlation between the catalytic activity and the number, type, and strength of the surface acid sites on Ga₂O₃-NR and γ -Ga₂O₃-lit was studied by temperature programmed desorption (TPD) of adsorbed pyridine monitored by FTIR spectroscopy (Figure 2C and Table 1).^[5a,18] Lewis acid sites in gallium oxides are generally attributed to coordinatively unsaturated Ga³⁺ ions mainly located in tetrahedral sites on the surface,^[5a] whereas surface Ga–OH groups are responsible for mild Brønsted acidity. These Brønsted acid sites can convert into Lewis acid sites by surface dehydration upon treatment at high temperature and tend to reconvert to Brønsted acid sites by rehydration at room temperature.^[19] Ga₂O₃-NR displays a much higher number of acid sites per gram of catalyst compared to γ -Ga₂O₃-lit (Table 1). This significant difference stems from the combination of two parameters: the higher surface area of Ga₂O₃-NR, and its higher surface density of acid sites (Table 1). Both these

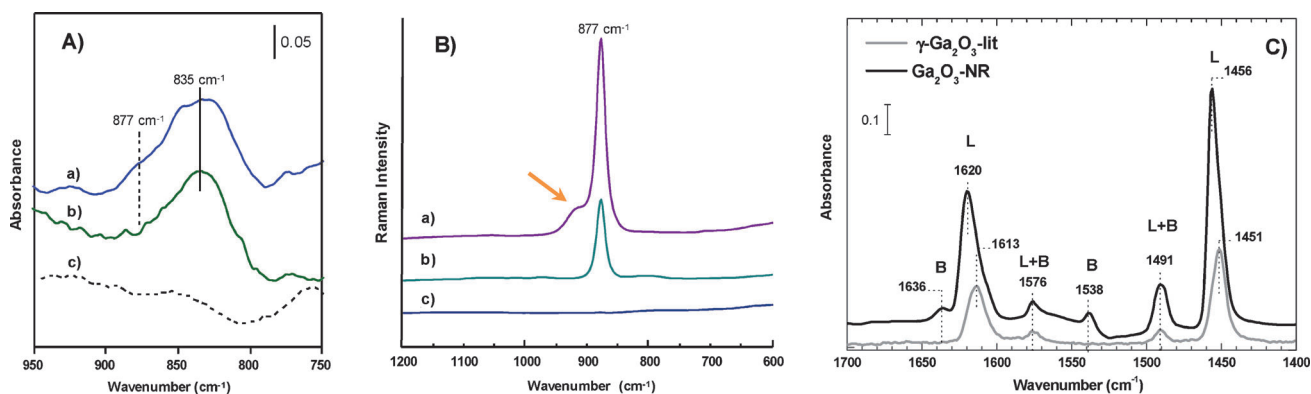
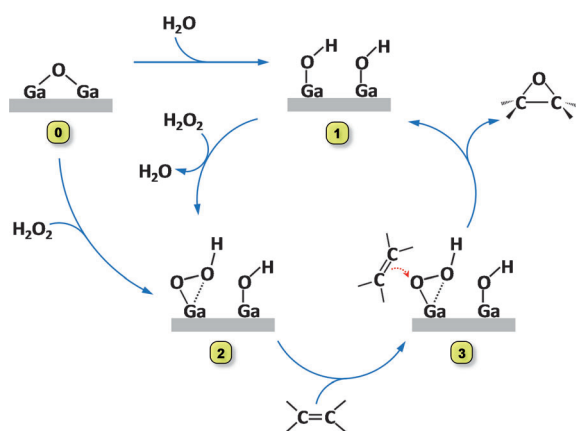


Figure 2. A) FTIR difference spectra of: a) Ga₂O₃-NR impregnated with 30 wt% aqueous H₂O₂, collected at nominal temperature of –173 °C; b) after 10 h evacuation at RT; c) Ga₂O₃-NR impregnated with H₂O. The spectrum of pure Ga₂O₃-NR evacuated at RT was subtracted from all spectra. The shoulder at 877 cm⁻¹ in (a) is ascribed to residual physisorbed H₂O₂, which is removed upon evacuation and heating from –173 °C to RT. In agreement with the observed signal in the IR spectrum, Ga₂O₃-NR is able to activate H₂O₂ towards the epoxidation of cyclooctene also at 25 °C (though with lower yield, 5% after 24 h). B) Raman spectra of: a) Ga₂O₃-NR impregnated with 50 wt% aqueous H₂O₂; b) SiO₂ impregnated with 50 wt% aqueous H₂O₂; c) Ga₂O₃-NR impregnated with H₂O. The arrow indicates the shoulder appearing in the Ga₂O₃-NR/H₂O₂/H₂O spectrum. C) FTIR spectra of pyridine chemisorbed on Ga₂O₃-NR and on γ -Ga₂O₃-lit (measured at 150 °C). L and B indicate pyridine adsorbed on Lewis and Brønsted acid sites, respectively. See Figure S5 for the evolution of the spectrum on Ga₂O₃-NR as a function of temperature.

features originate from the nanorod morphology of the catalyst: the higher surface area is a consequence of the higher surface-to-volume ratio of nanosized materials, whereas the higher surface density of acid sites is attributed to the intrinsically defective nature of the nanorods and the consequent higher density of coordinatively unsaturated sites on their surface compared to materials consisting of larger particles. Moreover, the Lewis acid sites in Ga_2O_3 -NR are stronger than those in $\gamma\text{-Ga}_2\text{O}_3$ -lit, as proven by the shift to higher wavenumbers of the peaks originating from pyridine adsorbed on this type of acid sites (Figure 2C).^[5a,18] This is in line with the higher chemical shift of the ^{71}Ga NMR signal of tetrahedral Ga sites in Ga_2O_3 -NR compared to $\gamma\text{-Ga}_2\text{O}_3$ -lit (Figure 1G).

On the basis of these characterization data, a catalytic mechanism for the epoxidation of alkenes over Ga_2O_3 -NR can be proposed (Scheme 1). Both coordinatively unsaturated



Scheme 1. Proposed catalytic cycle for the epoxidation of alkenes with aqueous H_2O_2 over Ga_2O_3 -NR.

Ga atoms acting as Lewis acid sites and mainly tetrahedral Ga-OH groups acting as mild Brønsted acid sites located at the surface of the nanorods can be considered as catalytic sites for the epoxidation reaction. Lewis acid sites that are present in the as-synthesized catalyst are expected to convert in contact with either H_2O or H_2O_2 during the epoxidation reaction ($0 \rightarrow 1$ and $0 \rightarrow 2$). These Ga sites are able to activate hydrogen peroxide (**2**), as indicated by FTIR and Raman spectroscopy. The observed stronger acidity of the Ga centers in Ga_2O_3 -NR compared to those in $\gamma\text{-Ga}_2\text{O}_3$ -lit enhances the polarization of the O–O bond of the hydroperoxide, thus favoring the electrophilic attack on the double bond of the alkene (**3**),^[20] which leads to the transfer of an oxygen atom with formation of the desired epoxide product.

The turnover numbers (TON) over Ga_2O_3 -NR were calculated based on the number of acid sites determined by TPD-FTIR (Table 2). High TONs were reached in the epoxidation of all tested alkenes, with a maximum value for cyclooctene (266). Moreover, the productivity of Ga_2O_3 -NR (Table 2) is more than double compared to previously reported transition-metal-free oxide catalysts.^[16b] These data confirm the outstanding catalytic properties of Ga_2O_3 -NR,

which is competitive against the industrial benchmark TS-1 with a terminal linear alkene as 1-octene but is much more versatile as its nanorod open structure allows the efficient epoxidation of larger substrates.

The truly heterogeneous character of Ga_2O_3 -NR was demonstrated by a hot-filtration test, which ruled out leaching of catalytically active species during the epoxidation. No acetic acid was detected by gas chromatography (GC) at the end of the catalytic tests, thus excluding hydrolysis of ethyl acetate, which could have contributed to the epoxidation activity as acetic acid can act as homogeneous catalyst through the formation of a peracid upon reaction with H_2O_2 .^[21] Ga_2O_3 -NR retained most of its activity upon recycling in five consecutive catalytic runs (Figure S6). This represents a remarkable improvement compared to other transition-metal-free epoxidation catalysts, which suffer from relatively rapid deactivation.^[16,22] Ga_2O_3 -NR was also more efficient in the use of H_2O_2 compared to other transition-metal-free oxides and to TS-1 (see the Supporting Information).^[16,22]

In summary, we introduced a template-free, straightforward method for the synthesis of gallium oxide nanorods with very high specific surface area and uniquely small dimensions compared to previously reported one-dimensional gallium oxides.^[1] Ga_2O_3 -NR displays excellent catalytic performance in the sustainable epoxidation of alkenes with H_2O_2 , achieving high efficiency in terms of activity, selectivity, oxidant consumption, substrate versatility, and recyclability. The attractive features of Ga_2O_3 -NR are very promising for a broad range of other relevant applications of gallium oxide that could benefit from a nanorod morphology, both within catalysis and as functional material with semiconducting, optoelectronic or sensing properties.^[23]

Received: September 25, 2013

Revised: November 14, 2013

Published online: January 22, 2014

Keywords: epoxidation · gallium oxide · heterogeneous catalysis · hydrogen peroxide · nanorods

- [1] a) G. R. Patzke, F. Krumeich, R. Nesper, *Angew. Chem.* **2002**, *114*, 2554; *Angew. Chem. Int. Ed.* **2002**, *41*, 2446; b) Y. Jun, J. Choi, J. Cheon, *Angew. Chem.* **2006**, *118*, 3492; *Angew. Chem. Int. Ed.* **2006**, *45*, 3414.
- [2] G. R. Patzke, Y. Zhou, R. Kontic, F. Conrad, *Angew. Chem.* **2011**, *123*, 852; *Angew. Chem. Int. Ed.* **2011**, *50*, 826.
- [3] C. Otero Areán, A. L. Bellan, M. P. Mentrut, M. R. Delgado, G. T. Palomino, *Microporous Mesoporous Mater.* **2000**, *40*, 35.
- [4] H. Y. Playford, A. C. Hannon, E. R. Barney, R. I. Walton, *Chem. Eur. J.* **2013**, *19*, 2803.
- [5] a) A. Vimont, J. Lavalley, A. Sahibed-Dine, C. O. Areán, M. R. Delgado, M. Daturi, *J. Phys. Chem. B* **2005**, *109*, 9656; b) C. Aprile, E. Gobechiya, J. A. Martens, P. P. Pescarmona, *Chem. Commun.* **2010**, *46*, 7712.
- [6] a) For example, the cell parameters of boehmite, $\gamma\text{-AlO}(\text{OH})$, are $a = 3.700$, $b = 12.227$, $c = 2.868$ Å, [00-021-1307]; b) P. A. Buining, C. Pathmamanoharan, J. B. H. Jansen, H. N. W. Lekkerkerker, *J. Am. Ceram. Soc.* **1991**, *74*, 1303.
- [7] X. Krokidis, P. Raybaud, A. E. Gobichon, B. Rebours, P. Euzen, H. Toulhoat, *J. Phys. Chem. B* **2001**, *105*, 5121.

- [8] D. Tunega, H. Pašalić, M. Gerzabek, H. Lischka, *J. Phys. Condens. Matter* **2011**, 23, 404201.
- [9] a) S. T. Oyama, *Mechanisms in homogeneous and heterogeneous epoxidation catalysis*, Elsevier Science, Amsterdam, **2008**; b) B. S. Lane, K. Burgess, *Chem. Rev.* **2003**, 103, 2457.
- [10] a) F. Cavani, J. H. Teles, *ChemSusChem* **2009**, 2, 508; b) W. Fan, R. G. Duan, T. Yokoi, P. Wu, Y. Kubota, T. Tatsumi, *J. Am. Chem. Soc.* **2008**, 130, 10150.
- [11] K. Lin, P. P. Pescarmona, K. Houthoofd, D. Liang, G. Van Tendeloo, P. A. Jacobs, *J. Catal.* **2009**, 263, 75.
- [12] V. Hulea, E. Dumitriu, *Appl. Catal. A* **2004**, 277, 99.
- [13] a) S. Bordiga, A. Damin, F. Bonino, G. Ricchiardi, C. Lamberti, A. Zecchina, *Angew. Chem.* **2002**, 114, 4928; *Angew. Chem. Int. Ed.* **2002**, 41, 4734; b) S. Bordiga, F. Bonino, A. Damin, C. Lamberti, *Phys. Chem. Chem. Phys.* **2008**, 10, 4854.
- [14] W. Lin, H. Frei, *J. Am. Chem. Soc.* **2002**, 124, 9292.
- [15] I. Arends, R. Sheldon, *Top. Catal.* **2002**, 19, 133.
- [16] a) R. Rinaldi, U. Schuchardt, *J. Catal.* **2004**, 227, 109; b) G. Stoica, M. Santiago, P. A. Jacobs, J. Pérez-Ramírez, P. P. Pescarmona, *Appl. Catal. A* **2009**, 371, 43.
- [17] C. Özdilek, K. Kazimierczak, S. J. Picken, *Polymer* **2005**, 46, 6025–6034.
- [18] G. Busca, *Phys. Chem. Chem. Phys.* **1999**, 1, 723.
- [19] P. Atkins, T. Overton, J. Rourke, M. Weller, F. Armstrong, *Inorganic chemistry*, 4th ed., Oxford University, Oxford, **2006**, p. 695.
- [20] K. Neimann, R. Neumann, *Org. Lett.* **2000**, 2, 2861.
- [21] H. Yao, D. E. Richardson, *J. Am. Chem. Soc.* **2000**, 122, 3220.
- [22] a) D. Mandelli, M. C. A. van Vliet, R. A. Sheldon, U. Schuchardt, *Appl. Catal. A* **2001**, 219, 209; b) P. P. Pescarmona, K. P. F. Janssen, P. A. Jacobs, *Chem. Eur. J.* **2007**, 13, 6562.
- [23] a) V. R. Choudhary, S. K. Jana, B. P. Kiran, *J. Catal.* **2000**, 192, 257; b) K. Nakagawa, M. Okamura, N. Ikenaga, T. Suzuki, T. Kobayashi, *Chem. Commun.* **1998**, 9, 1025; c) X. Wang, Q. Xu, M. Li, S. Shen, X. Wang, Y. Wang, Z. Feng, J. Shi, H. Han, C. Li, *Angew. Chem.* **2012**, 124, 13266; *Angew. Chem. Int. Ed.* **2012**, 51, 13089.